



Contents lists available at *Dergipark*

## Journal of Scientific Reports-A

journal homepage: <https://dergipark.org.tr/pub/jsr-a>



**E-ISSN: 2687-6167**

**Number 55, December 2023**

### RESEARCH ARTICLE

Receive Date: 02.10.2023

Accepted Date: 21.12.2023

## Positioning analysis of the lift force sensor in subsonic wind tunnel test chamber design and its effect on naca0015 airfoil

Samet Giray Tunca<sup>1\*</sup>, Mustafa Arif Özgür<sup>2</sup>

<sup>1</sup>Kütahya Dumlupınar University, Kütahya Evliya Çelebi Campus, Kütahya, 43000, Türkiye, ORCID: 0000-0002-7632-8745

<sup>2</sup>Kütahya Dumlupınar University, Kütahya Evliya Çelebi Campus, Kütahya, 43000, Türkiye, ORCID: 0000-0001-5877-4293

### Abstract

In this study, analysis was carried out by placing the force sensor in different positions in the subsonic wind tunnel test room. NACA0015 profile was used as the airfoil. The model used in the open system subsonic wind tunnel with a 50x50 cm test chamber was manufactured by 3D printing method. Lift force (CL) measurements were studied at Reynolds number (Re) values of 60000, 80000 and 100000. Measurements were analyzed in one-degree increments of the angle of attack, starting from 0°. The force device is positioned in 4 different ways around the test room. Efficient results could not be obtained in 3 of the connection attempts. The reason why the results are not efficient is that the fasteners are incompatible with the airfoil, force device and system. The incompatibility of the fasteners caused vibration and a negative situation in the airfoil. There is a slope in the connection made from the side. As a result of the slope, the airfoil has deteriorated.

It was observed that the measurements made by positioning the force device inside the test chamber were compatible with the literature. The resulting graph shows an approach to the literature. Although it is graphically compatible, it should be noted that there is a deviation of approximately 10% in the data. Connection stiffness is gaining importance. It has been observed that stall begins at angles of approximately 10° and 11° degrees.

Improvements can be made for all connections and fasteners for the location of the force device.

© 2023 DPU All rights reserved.

**Keywords:** Wind tunnel, stall, airfoil, lift coefficient, Reynolds number

\* Corresponding author. Tel.: 0 274 443 71 00  
E-mail address: [sgiray.tunca@dpu.edu.tr](mailto:sgiray.tunca@dpu.edu.tr)  
<http://dx.doi.org/10.1016/j.cviu.2017.00.000>

## 1. Introduction

Experimental aerodynamic measurements are made using wind tunnels. There are many studies conducted with wind tunnels in the literature. The work to be done must comply with the characteristics of the wind tunnel. At the same time aerodynamic measurements are made to determine the characteristic structures of airfoils. These measurements are used to optimize the structure of the airfoil. Lift coefficient values are taken into consideration to examine the condition of the airfoil during takeoff, flight and landing. The airfoil is evaluated by making comparisons with studies performed at different angles. In the literature, there are many studies examining airfoil and making aerodynamic measurements.

Aeroacoustic measurements were made on two NACA 0012 airfoil sections with different chord length and sharp trailing edge in the Laminar Wind Tunnel (LWT) of the University of Stuttgart [1].

Regarding wind tunnel manufacturing studies, a small, two-dimensional, high-speed cryogenic wind tunnel was built at the Japanese National Defense Academy (NDA) in 1985. R4 airfoil test results in the NDA cryogenic wind tunnel were compared to those of NASA TM-85739 [2].

In the study by Bottasso C.L. et al. on wind tunnel modeling, it was stated that the existing experimental facility, which expands the classical scope of the models, enables various applications from aerodynamics to aeroelasticity and control [3].

Power coefficient and torque coefficient parameters were examined for the disc-shaped wind rotor used in a small-scale wind turbine. Data were obtained by numerical simulation and wind tunnel testing. It was simulated with different turbulence models in the range of Re numbers  $6.8 \times 10^4$ – $1.70 \times 10^5$  [4].

Göv I. The study by et al. was based on the NACA 4412 airfoil. Changes have been made to the NACA 4412 profile to provide higher aerodynamic performance at 0-23 degree angles of attack during flight. Two more different airfoil profiles (NACA 4412\_1 and NACA 4412\_2) were obtained. The aerodynamic performances of these two profiles and the original NACA 4412 profile were compared. In these analyses, lift coefficient, drag coefficient and flow separation performance parameters were examined. At the end of the study, it was determined that it was appropriate to use the NACA 4412 airfoil between  $0^\circ$  and  $12^\circ$ , the NACA 4412\_2 airfoil between  $12^\circ$  and  $17^\circ$ , and the NACA 4412\_1 airfoil after  $17^\circ$  angle of attack in order to achieve maximum aerodynamic efficiency [5].

In the research of Du G. et al., airfoil lift, drag and lift-drag ratios were studied with numerical simulation analysis and their variables were analyzed in different parameters of NACA airfoils [6].

Rubel R.I. et al. used a symmetrical airfoil profile (NACA 0015) in their study. This airfoil is used in many applications such as aircraft submarine winglets, rotary and some fixed wings. In the study, NACA 0015 was examined numerically and experimentally in the range of  $0^\circ$  -  $18^\circ$ . The aim of the study is to find the deviation and validity of the aerodynamic properties of the NACA 0015 airfoil for experimental and numerical method [7].

The vortex structure of the NACA 0018 airfoil was examined at  $2.5 \times 10^4$  number and angles of attack of  $10^\circ$  and  $20^\circ$  by Gim O. and Lee G. Velocity profiles were obtained [8].

In wind tunnel tests, the vibration of the NACA0015 airfoil in the range of  $18 \times 10^4$  and  $57 \times 10^4$  Reynolds number was investigated. As a result of this research, flow visualization was realized [9].

A comparison was made between the performance of the symmetrical airfoil NACA-0012 and the asymmetric airfoil NACA-2410. The relationship between CL and CD has been explained. It can be seen that the lift and drag coefficient of NACA-0012 is higher than that of NACA-2410 [10].

Wind tunnel tests were performed on the NACA 0012 two-dimensional airfoil. The measurements taken referred to the pressure distribution on an airfoil and airfoil coefficients using six-component balance between  $0^\circ$  and  $18^\circ$  degrees angle of attack, and investigations at small angles of attack [11].

A set of 15 different corona actuators with triangular tips on their anodes were examined by mounting them on the leading edge of the NACA 0015 airfoil. Aerodynamic forces on the airfoil are measured over a wide range of angles of attack for different airflow velocities in the wind tunnel. The performance of the actuators was evaluated through various parameters, including critical and average lift increase, resistance reduction and power saving effectiveness [12].

Angular airfoil were tested in a subsonic wind tunnel at numbers lower than  $2 \times 10^4$  Reynolds number. CL and CD

tests of the NACA0012 airfoil were compared with thin and curved structures. It has been determined that the most ideal airfoil at Reynolds numbers up to  $7 \times 10^4$  is a circular structure with 5 percent. This structure provided the highest CL-CD figures across all turbulence levels [13].

New data have been obtained for the NACA-0012 airfoil at low Reynolds numbers for the analysis of vertical axis wind turbines (VAWTs). The double-slat tolerant tunnel has the best performance based on the similarity of results for the airfoils. However, post-stall force peaks are significantly lower than in conventional tunneling [14].

The lift coefficient of a NACA 0015 airfoil with and without a Gurney airfoil was examined in a wind tunnel with  $Re = 2.0 \times 10^5$ . The Gurney wing provided a significant and relatively constant increase in lift throughout the linear range of the CL versus  $\alpha$  curve [15].

It was determined that the results obtained in the study conducted by Kaya M. coincide with the results of wind tunnel experiments carried out by many research units such as NACA [16]. Miklosevic studied aerodynamic force calculations in a low-speed wind tunnel at Reynolds numbers between 505,000 and 520,000 and angles of attack varying between  $-2^\circ$  and  $20^\circ$  [17].

H. Hamdani and M. Sun's study with the NACA 0012 airfoil shows that at low Reynolds numbers, the instantaneous acceleration of the airfoil from one speed to another causes large aerodynamic forces to arise [18].

Kazemi examined the aerodynamic performances of the airfoil they produced numerically and experimentally. They stated that the lift/drag ratio increased approximately 2.9 times compared to the NACA0021 airfoil, which they accepted as the basis for the profile structure they produced [19].

In their study, Tanürün H. E., Ata İ., Yaşam M. E. and Acır A compared the experimental results of the aerodynamic performance of the NACA0018 airfoil with two newly designed airfoil. In the aerodynamic experimental results of the newly designed AR1 and AR2 airfoil, an improvement of 0.41% and 2.71% in CL values was achieved [20].

In our study, the ambient temperature was  $20^\circ\text{C}$ , the kinematic viscosity of the air was accepted as  $1.5111 \times 10^{-5} \text{ m}^2/\text{s}$ , and the airfoil chord length was 0.15 m. Tests were carried out at Re numbers of  $6 \times 10^4$ ,  $8 \times 10^4$  and  $10 \times 10^4$ .

The location of the force measurement system is important in experimental studies. However, the connection of the airfoil and the force device is important for the accuracy of the data obtained. In our study, experiments were carried out with different methods to determine the position of the force system. Among these methods, there are also experiments in which the connection between the airfoil and the force device varies. The results obtained will be considered as a reference for future experiments in the subsonic wind tunnel. There is a metal flat piece between the sensor in the force device and the airfoil. For this reason, it has been determined that the force device should be on the airfoil axis.

## 2. Experimental studies and evaluation

There is an open system subsonic wind tunnel in Kütahya Dumlupınar University Mechanical Engineering Laboratory (Fig. 1.). The test compartment where the airfoil to be tested is placed is 50x50 cm. In our study, buoyancy measurements were obtained from many different locations and with different connection methods.



Fig.1. Subsonic Wind Tunnel

NACA0015 airfoil was used in lift force measurements made with the wind tunnel force balancing system. The airfoil and fasteners were manufactured on a 3D printer. Due to vibration, metal fasteners were also tested in the measurements.

To manufacture the airfoil, printing parameters were determined as 220<sup>0</sup> nozzle temperature, 60 degree table temperature and 0,2 mm layer thickness. The material used is pla filament. For airfoil printing, the ratio of airfoil length and chord length is accepted as 1/1. The airfoil mass was manufactured as 348,21 g, volume as 341379,35 mm<sup>3</sup> and surface area as 54582 mm<sup>2</sup>.

The connection elements between the force device and the airfoil are important for the accuracy of the data in the experiments. In order for the fasteners to be connected rigidly, the airfoil section must be of a certain thickness. Therefore the chord length measurement is 150 mm. was determined as.

Lift force values were taken in the wind tunnel test chamber. The studies were carried out at speeds of 6, 8 and 10 m/s, in increments of 1<sup>0</sup> between 0<sup>0</sup> - 14<sup>0</sup> degrees. The chord length of the NACA0015 airfoil used in the tests is 150 mm. The area where the lift force acts is the lower part of the airfoil surface. The lift coefficient was obtained along with the speed and density values.

### 2.1. Mathematical model

Terms used in aerodynamic studies have mathematical equivalents. The terms used in the calculations made in our study were obtained with these mathematical formulas.

- The term subsonic is expressed in Mach number. In fluid mechanics, Mach number is the ratio of the speed of a moving mass to the speed of sound under the conditions in which the mass exists.  $V$  (m/s) refers to the speed of the mass in motion, and  $c$  (m/s) refers to the speed of sound.

$$Ma = V/c \quad (1)$$

$V$  (m/s) refers to the speed of the mass in motion, and  $c$  (m/s) refers to the speed of sound. Situations where the Mach number is less than 0.8 are called subsonic.

- The buoyant force acts on the object perpendicular to the flow.

$$FL = CL \frac{1}{2} \rho AV^2 \quad (2)$$

CL is the dimensionless drag force coefficient,  $\rho$  ( $\text{kg/m}^3$ ) is the density of the air, A ( $\text{m}^2$ ) is the area of influence of the wind on the airfoil, and V (m/s) is the wind speed.

- In fluid mechanics, Reynolds number (Re) is the ratio of a fluid's inertial forces (v,d) to viscosity forces ( $\mu/\rho$ ). In our study, tests were conducted at three different Reynolds numbers.

$$Re = \frac{(v.d.\rho)}{\mu} \quad (3)$$

- Stall is a term used in aerodynamics. When stall occurs, the lift acting on the airfoils suddenly and unexpectedly decreases or disappears completely. The aerodynamic angle at which the maximum lift coefficient is reached or dropped below is called the "stall angle". As a result of the separation of the air flow on the airfoil surfaces or the flow becoming turbulent, the amount of lift that the airfoils can produce decreases. While the airfoils normally operate aerodynamically at a certain angle, when this angle is exceeded or approached with sudden changes, the air flow becomes irregular and lift decreases.

## 2.2. Force sensor connection from the rear area of the airfoil

In the first connection method, the device is positioned at the rear of the NACA0015 airfoil with a connecting rod coming from the rear region of the airfoil. The airfoil is manufactured as shown in figure 2. The measurement results are as seen in Figure-3. There is no stall in the measurement results. The fact that no stall is observed with such a measurement method is due to the fact that the connection part in the back region affects the force values. As seen in figure-3, lift force values are constantly increasing. Measurements were tested at different angles by making a connection in the back area, but the result did not change. Although the angle mechanism part was positioned close and far from the rear section, the increase in lifting force could not be prevented and no stall was observed.

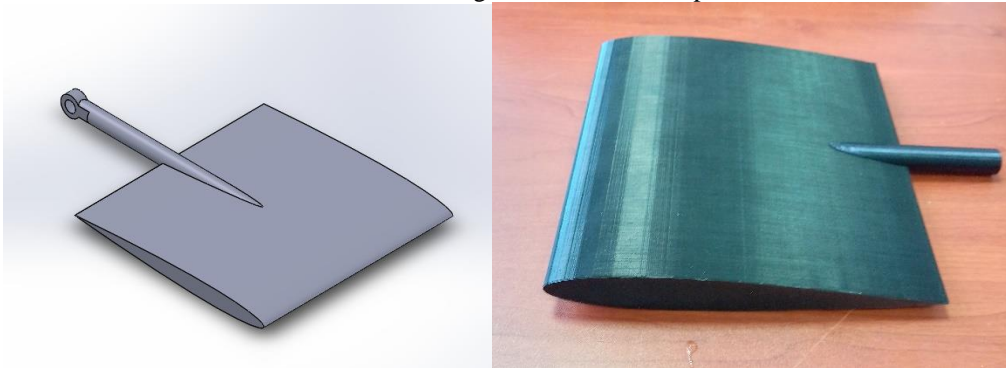


Fig. 2. Airfoil and connection used in the measurement made from the rear area of the airfoil

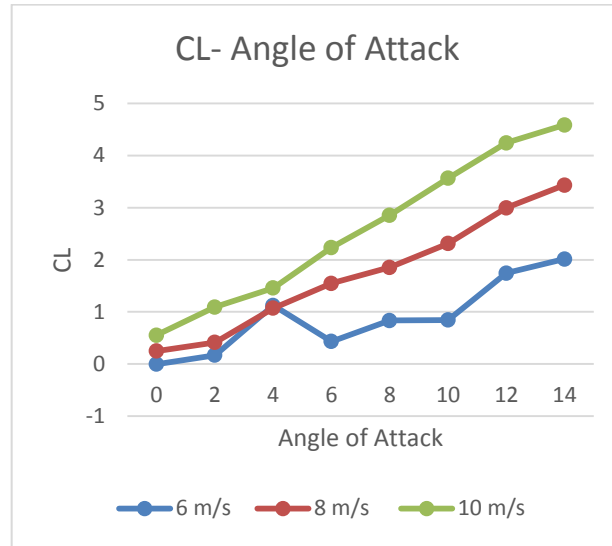


Fig. 3. NACA0015 airfoil lift coefficient (CL) and angle of attack graph (*Force Sensor Connection from the Rear Area of the Airfoil*)

Experiments were carried out with rear connection as the first method in Figure 3. The increase in the distance between the sensor airfoil is the reason for the high distribution of moment arm values created by these formations. The  $6 \times 10^4$  Re view CL maximum value increased to 2, the  $8 \times 10^4$  Re view CL maximum value increased to 3,43 and the  $10 \times 10^4$  Re view CL maximum value increased to 4,588. These values do not match the literature. The blocking effect of speed and openness is observed. The airfoil is not exposed to stall and there is a continuous increase in CL values.

### 2.3. Force sensor connection at the bottom outside of the test chamber

As the second connection method, the device was placed under the test chamber. The device was placed on the same axis as the airfoil but outside the test chamber to avoid causing any different effects on the flow. There are 2 -  $90^0$  turns in the connection between the device and the airfoils. However, with the positioning, the distance between the airfoil and the device was extended and negative situations were encountered in load transfer. The buoyancy data obtained are very low compared to literature data. With this connection type, no stall was observed. As in the first connection method, the connection was made on the same axis from the back region. It has become clear that the connections applied to the airfoil in this way have an effect on preventing stall. The data obtained from the connections made to the airfoil from the rear area to the force device are not positive.

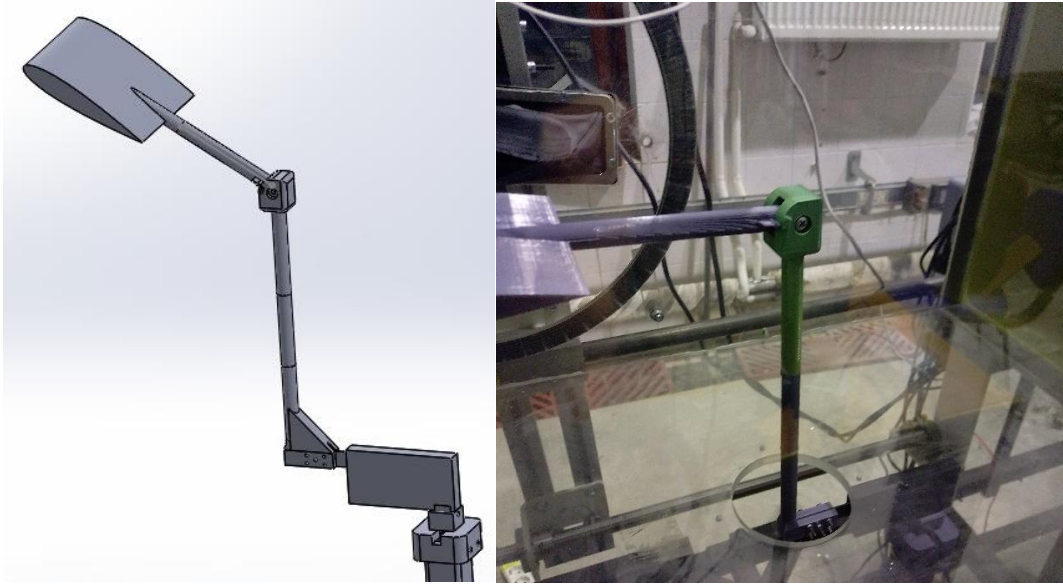


Fig. 4. Airfoil and connection used in the measurement made from the rear area of the airfoil outside the test room

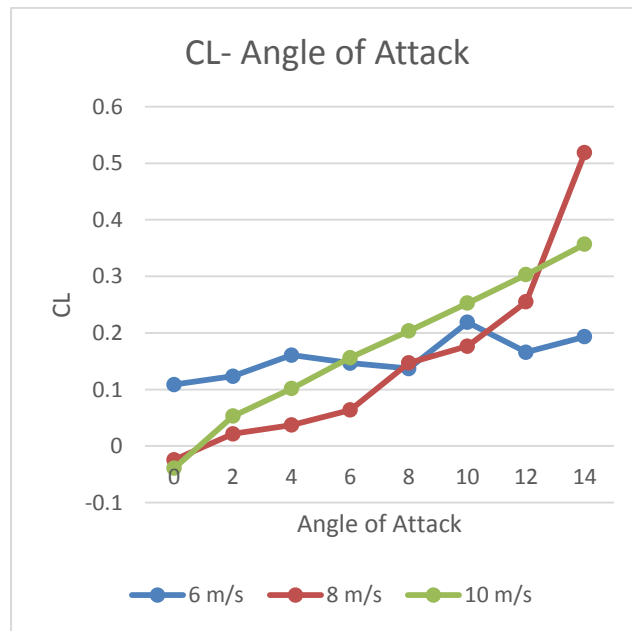


Fig. 5. NACA0015 airfoil lift coefficient (CL) and angle of attack graph (*Force Sensor Connection at the Bottom Outside of the Test Chamber*)

In the method shown in Figure 4, the force device is positioned very far from the airfoil. As seen in Figure 5, the data obtained is very low. In measurements where the Re number was  $8 \times 10^4$ , the maximum CL value was found to be 0,5186. There is no consistency between measurements made with the same method at 3 different Re numbers.

The  $90^\circ$  rotations and distance between the force device and the airfoil caused losses in force values. Likewise, it

has been determined that this method has high vibration.

#### 2.4. Force sensor connection from side of test chamber

In this method, the device is positioned on the outer side of the test chamber and a connection is made from the side surface of the airfoil. Since the connection was one-sided, the requested data could not be obtained. As seen in Figure 6, in the connection made, the force acting on the airfoil created a force in the opposite direction on the flat iron, which is the device sensor connection element. In addition, since it is a one-sided connection, the slope and vibration have increased meaninglessly. As a result, no data could be obtained from this connection.

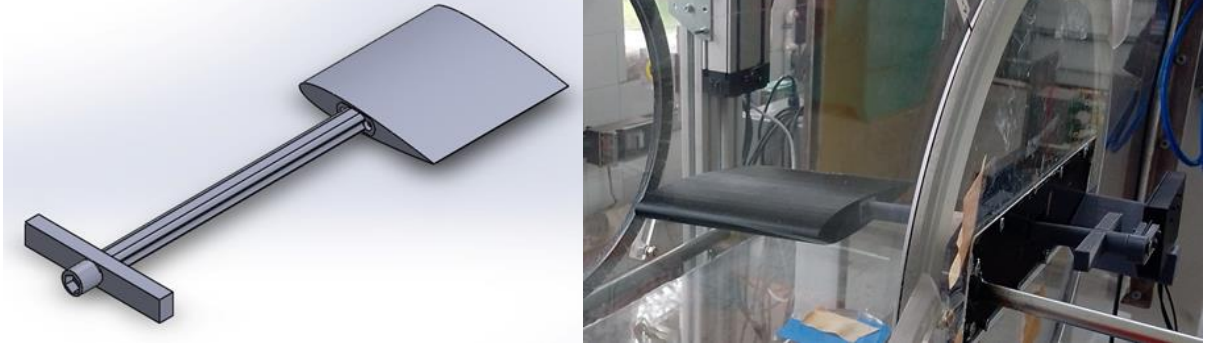


Fig. 6. Airfoil and connection used in the measurement made from the side area of the airfoil

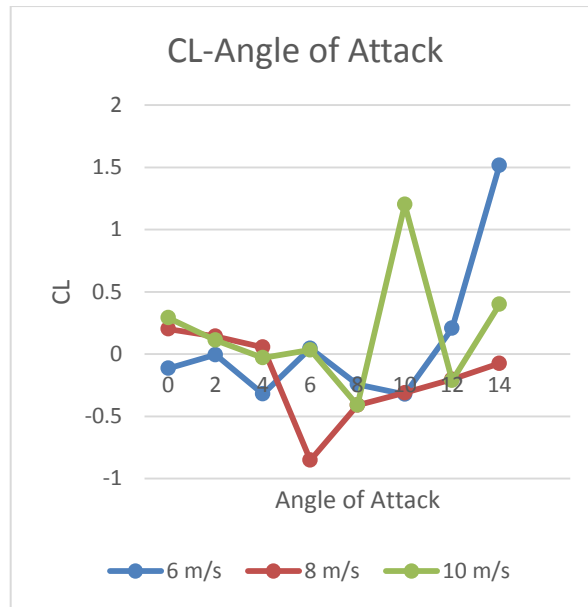


Fig.7. NACA0015 airfoil lift coefficient (CL) and angle of attack graph (Force Sensor Connection from Side of Test Chamber)

As a result of the experiments, the data in Figure 7 was obtained. Due to the one-sided connection, the wind



speed affecting the angled wing profile created a downward force at the connection point with the force device. This force has no continuity. Some of the measurements were negative and some were positive. In the data obtained, the maximum value of CL increased up to 1,5. However, the CL minimum value was between -0,5 and -1. As a result, it has been determined that this method is not a suitable method for comparing experimental data with the literature.

### 2.5. Force sensor connection at the bottom of the test chamber

In the last method applied in this study, the force device was fixed to the inner floor of the test chamber. As seen in Figure 8, the airfoil device connection design has been made. A stall effect is observed in the lift coefficient values obtained with this method. Although the values overlap with literature studies, it has been determined that there are losses in buoyancy values.

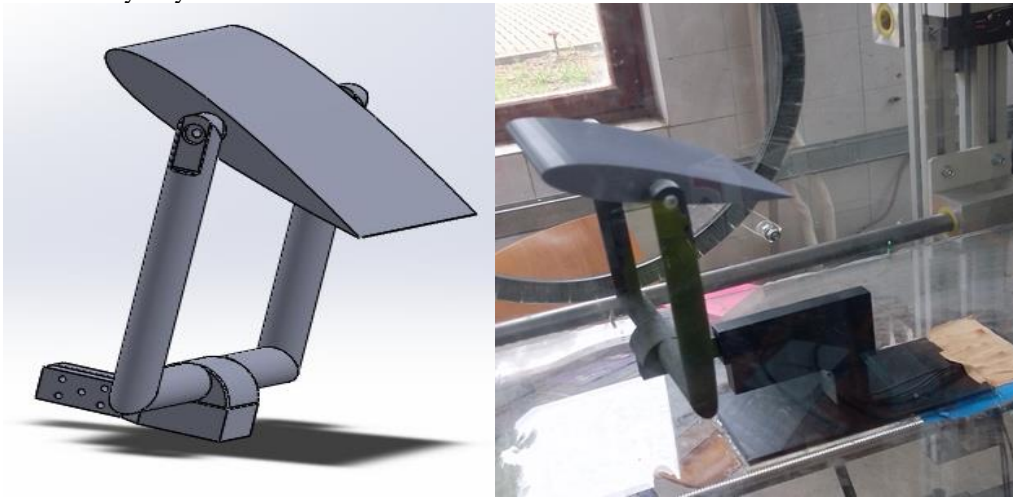


Fig. 8. Force device positioned under the airfoil, airfoil and connection

## 3. Results

Stall was detected in the connection made under the Naca0015 profile (Table 1.). Increases removal permanent values up to  $11^{\circ}$ . After completing  $11^{\circ}$ , it is seen that there is a decrease in the lifting force of the airfoil. When compared with the literature, it is revealed that there are losses in the total lifting values in Table 1. Our study has been presented to the literature as graphic curves.

Measurements were made at different speeds in the wind tunnel. It is seen that vibration has an effect on the values measured at 10 m/s speed. The result of this can be seen in the graph (Fig.9.)

In Fig. 9, lift coefficient values are given for angles of attack from 0 to  $13^{\circ}$  degrees. These measurements were made at speeds of 6, 8 and 10 m/s.

Table 1. Lift Coefficient (CL) values

Angle of Attack	Vel (m/s)		
	6 (m/s)	8 (m/s)	10 (m/s)
<b>0</b>	0,009213	0,015078	0,001254
<b>1</b>	0,051821	0,150776	0,016643
<b>2</b>	0,108962	0,156389	0,096507
<b>3</b>	0,159917	0,189557	0,156826
<b>4</b>	0,210872	0,225804	0,187386
<b>5</b>	0,228533	0,264769	0,184223
<b>6</b>	0,288234	0,304067	0,223396
<b>7</b>	0,31356	0,362659	0,425558
<b>8</b>	0,379124	0,413702	0,477638
<b>9</b>	0,441421	0,44204	0,528705
<b>10</b>	0,539058	0,579669	0,626791
<b>11</b>	0,544485	0,614894	0,638808
<b>12</b>	0,414965	0,438963	0,563353
<b>13</b>	0,498562	0,501032	0,45656

Table 1. shows that there is a linear increase up to 11<sup>0</sup> degrees, and after this degree the airfoil is subject to stall. When the studies conducted with the NACA0015 airfoil were examined, it was determined that the coefficient values we obtained were low by 10%. It is thought that this situation is caused by loads shifting to the connection points.

When the connection methods used in our study were examined, it was understood that the force sensor should be on the same axis with the airfoil at the trailing edge.

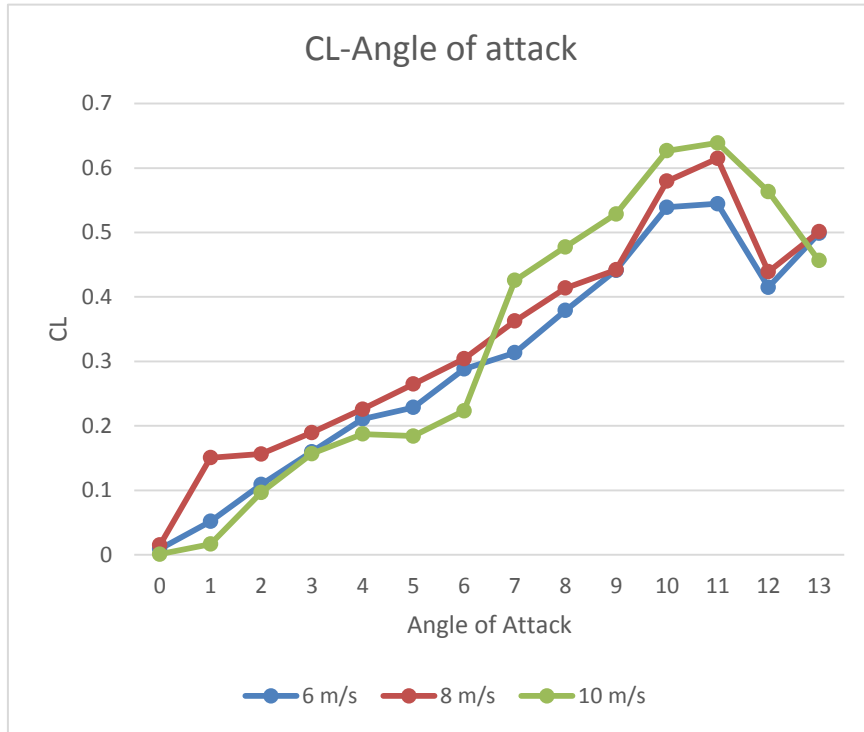


Fig. 9. NACA0015 airfoil lift coefficient (CL) and angle of attack graph

It seems that the method in heading 2.4 should be studied first for the lift coefficient values. Based on the results obtained, the studies continued and the necessity of improvement studies was determined. When the graph is examined, it is seen that there may be connection-related vibrations at 10 m/s measurements. Studies need to be done on this issue.

Güler A.A. conducted experiments with the Naca0015 airfoil at  $8,6 \times 10^4$  Re number. He carried out his study with angle of attack increments of  $2^0$ . It was observed that the Naca0015 airfoil entered a stall at  $10^0$  degrees. In the experiment, the maximum CL value was found to be 0,8 [21]. The stall angle in our study appears to be compatible with this study. Pope A. made his work in the number  $23 \times 10^4$  Re. It has been observed that the NACA0015 airfoil enters a stall between  $10^0 - 15^0$  degrees [22].

It has been understood that the results of other methods other than the Figure 8 method have no equivalent in the literature.

When the studies conducted with the NACA0015 airfoil were examined, it was determined that the coefficient values we obtained were low by 10%. It is thought that this situation is caused by loads shifting to the connection points.

#### 4. Discussions

Force losses can be eliminated with new connection designs. When the connection methods used in our study were examined, it was understood that the force sensor should be on the same axis with the airfoil at the trailing edge. Better efficiency can be achieved by changing the fasteners and system.

CL values obtained in methods other than Figure 8 are different from the literature. For this reason, these methods should not be preferred in future experiments. In some measurement results, it is seen that CL data is at negative values. Under normal conditions, the CL value should be seen as positive values in these experiments.

As the first method, experiments were carried out with a rear connection manufactured as in Figure 2. The distance between the sensor airfoil increased, and therefore the resulting moment arm caused the values to be high. In this method, as the angle increased, a blocking effect was observed on the wing. It can be seen in Figure 3 that the airfoil is not subjected to stall.

In the method shown in Figure 4, a connection is made on the rear axis. The device was taken out of the test chamber. In this method, the data obtained is low because the force device is too far away from the airfoil. There are turns in the connection system, so force losses occurred as seen in Figure 5.

In the method shown in Figure 6, the airfoil is connected to the force device from its side surface. Due to the distance between the wing and the force device, deflection was observed in the wing profile towards the opposite direction of the connection. This situation caused variability in the results. The wind speed acting on the non-rigid wing profile created a downward force value at the connection point with the force device. As seen in Figure 7, there are negative values. Force data should not be negative in the experiments performed.

Studies need to be carried out to eliminate the 10% loss in the data obtained by the method closest to the literature data. It seems that the results can be more efficient if the connection rigidity is ensured.

To create the optimum test room design, an examination should be made under headings such as materials used, fasteners and positioning.

## Acknowledgements

This article benefited from the support of Kütahya Dumlupınar University Priority Area Project with project number 2021-26.

## References

- [1] B.Polgmann and W.Würz, Experiments in Fluids, Volume 54, article number 1556, 2013.
- [2] Y.Yamaguchi, Y.Nakauchi, M.Yorozu and T.Saito, «Preliminary airfoil testing experience in the NDA cryogenic wind tunnel,» %1 içinde "ICIASF '91", *International Congress on Instrumentation in Aerospace Simulation Facilities*, Rockville USA, 1991.
- [3] C. L. Bottasso, F. Campagnolo and V. Petrovic, *Wind tunnel testing of scaled wind turbine models: Beyond aerodynamics*, cilt Volume 127, Journal of Wind Engineering and Industrial Aerodynamics, 2014, pp. 11-28.
- [4] Z. X. et.al, *Experimental and numerical investigation on aerodynamic performance of a novel disc-shaped wind rotor for the small-scale wind turbine*, cilt Volume 175, Energy Conversion and Management, 2018, pp. 173-191.
- [5] İ. Göv, M. H. Doğru and Ü. Korkmaz, *Uçuş esnasında değiştirilebilir kanat profili kullanarak NACA 4412'nin aerodinamik performansının artırılması*, cilt 34, Ankara: Gazi Üniversitesi Mühendislik Mimarlık Fakültesi Dergisi, 2019, pp. 1109-1125.
- [6] G.-M. Du, J.-H. Chou and P.-K. Huang, *Application of Taguchi experimental method in the optimal design of the NACA cascades wing*, Taiwan, Puli: 2016 International Conference on System Science and Engineering (ICSSE), 2016.
- [7] R. I. Rubel, M. Uddin, M. Islam and M. Rokunuzzaman, *Numerical and Experimental Investigation of Aerodynamics Characteristics of NACA 0015 Aerofoil*, cilt Vol.2, International Journal of Engineering Technologies, 2016, pp. 132-142.
- [8] O.-S. Gim and G.-W. Lee, *Flow characteristics and tip vortex formation around a NACA 0018 foil with anendplate*, cilt Vol.60, Ocean Engineering, 2013, pp. 28-38.
- [9] P. Sidlof, V. Vlcek and M. Stepan, *Experimental investigation of flow-induced vibration of a pitch-plunge NACA 0015 airfoil under deep dynamic stall*, cilt Vol.67, Journal of Fluids and Structures, 2016, pp. 48-59.
- [10] S. Sarjito, *Studi Karakteristik Airfoil Naca 2410 Dan Naca 0012 pada Berbagai Variasi Angle Of Attack*, Media Mesin Majalah Teknik Mesin, 2010.
- [11] Michos A., Bergeles G. and Athanassiadis N., *Aerodynamic Characteristics of NACA 0012 Airfoil in Relation to Wind Generators*, cilt 7:4, United Kingdom: Wind Engineering, 1984, pp. 247-262.
- [12] M. Belan and F. Messanelli, *Wind tunnel testing of multi-tip corona actuators on a symmetric airfoil*, cilt Vol.85, Journal of Electrostatics, 2017, pp. 23-34.
- [13] E.V.Laitone, *Wind tunnel tests of wings at Reynolds numbers below 70 000*, cilt Vol.23, Experiments in Fluids, 1997, pp. 405-409.
- [14] J.M.Rainbird, J.Peiro and J.M.R.Graham, *Blockage-tolerant wind tunnel measurements for a NACA 0012 at high angles of attack*, cilt Vol.145, Journal of Wind Engineering and Industrial Aerodynamics, 2015, pp. 2019-218.
- [15] D.R.Troolin, E.K.Longmire and W.T.Lai, *Time resolved PIV analysis of flow over a NACA 0015 airfoil with Gurney flap*, cilt Vol.41,

Experiments in Fluids, 2006, pp. 241-254.

[16] M. Kaya, *Airfoil Yapının Yakın Çevresindeki Hız Ve Basınç Dağılımının Hesaplamalı Akışkanlar Dinamiği Yöntemi İle İncelenmesi*, Cilt %1 / %24-1, Erzincan: Erzincan Üniversitesi Fen Bilimleri Enstitüsü Dergisi, 2014, pp. 59-69.

[17] D. Miklosovic, M. Murray, L. Howle and F. Fish, *Leading-edge tubercles delay stall on humpback whale (Megaptera novaeangliae) flippers*, Cilt %1 / %216-5, Physics of Fluids, 2004, pp. L39-43.

[18] H. Hamdani and M. Sun, *Aerodynamic Forces and Flow Structures of an Airfoil in Some Unsteady Motions at Small Reynolds Number*, cilt Vol.145, Acta Mechanica, 2000, pp. 173-187.

[19] S. A. Kazemi, M. Nili-Ahmadabadi, A. Sedaghat and M. Saghafian, *Aerodynamic performance of a circulating airfoil section for Magnus systems via numerical simulation and flow visualization*, cilt Vol.104, Energy, 2016, pp. 1-15.

[20] H. E. Tanürün, İ. Ata, M. E. Canlı and A. Acır , *Farklı açıklık oranlarındaki NACA-0018 rüzgâr türbini kanat modeli performansının sayısal ve deneysel incelenmesi*, cilt 23, Politeknik Dergisi, 2020, pp. 371-381.

[21] A. A. Güler, *Naca0015 Model Uçak Kanadı Etrafındaki Akışın Plazma Aktüatör İle Aktif Kontrolünde Sinyal Modülasyonunun Deneysel İncelenmesi*, Niğde Ömer Halisdemir Üniversitesi Fen Bilimleri Enstitüsü, 2013.

[22] A. Pope, *The forces and moments over an NACA 0015 airfoil*, cilt Vol.58, Georgia Institute of Technology, Published in: Aero Digest, 1949.